Enzyme Kinetics and Binding Studies on Inhibitors of MEK Protein Kinase

Wendy S. VanScyoc,‡ Geoffrey A. Holdgate, Jane E. Sullivan, and Walter H. J. Ward*

AstraZeneca, Mereside, Alderley Park, Macclesfield, Cheshire SK10 4TG, U.K.

Received September 5, 2007; Revised Manuscript Received February 22, 2008

ABSTRACT: Inhibition of the protein kinase, MEK1, is a potential approach for the treatment of cancer. Inhibitors may act by prevention of activation (PoA), which involves interfering with phosphorylation of nonactivated MEK1 by the upstream kinase, B-RAF. Modulation also may occur by inhibition of catalysis (IoC) during phosphorylation of the downstream substrate, ERK2, by activated MEK1. Here, five MEK inhibitors are characterized in terms of binding affinity, PoA, and IoC. The compounds are a butadiene (U-0126), an *N*-alkoxy amide (CI-1040), two CI-1040 analogues (an anthranilic acid and an *N*-alkyl amide), and a cyanoquinoline. Some compounds give different mechanisms of inhibition (ATP-competitive, noncompetitive, or uncompetitive) in PoA compared to IoC or show a change in potency between the assays. The inhibitors also exhibit different shifts in potency when either PoA or IoC is compared with binding to nonactivated MEK. The inhibitor potency ranking, therefore, is dependent upon the assay format. When the ATP concentration equals K_m, IoC IC_{50} increases in the order CI-1040 ≈ cyanoquinoline < anthranilic acid ≈ U-0126 < alkyl amide. Conversely, the K_d from nonactivated MEK1 for four of the compounds varies between more than 6-fold lower and over 18-fold higher than this IC_{50}, with U-0126 having the lowest K_d and CI-1040 having the highest. In PoA when the ATP concentration equals K_m, U-0126 has the lowest IC_{50}, becoming more potent than CI-1040, the cyanoquinoline, and the anthranilic acid. These observations have implications for understanding structure–activity relationships of MEK inhibitors and illustrate how assays can be designed to favor different compounds.

The human genome encodes over 500 protein kinases (*1*), many of which are targets for inhibition during drug discovery (*2*). Most kinase inhibitors follow ATP-competitive kinetics, and some have been shown to occupy ATP-binding sites (*3, 4*). Optimization of compounds during drug discovery is assisted by an understanding of the relationship between structure and binding affinity. If the different compounds under consideration all follow ATP-competitive kinetics in the same kinase assay, then there is a correlation between the concentration required for 50% inhibition (IC_{50})[1] and the affinity for the target enzyme. Evaluation of selectivity may be complicated by different kinases having different affinities for ATP (*5*).

Around 30% of human tumors exhibit increased signaling through the mitogen-activated protein (MAP) kinase pathway, which has become a target for anticancer therapy (see refs *6* and *7*). The pathway is stimulated when a growth factor binds to a receptor tyrosine kinase, which then promotes the interaction of RAS with RAF, initiating a phosphorylation cascade through MAP kinase kinase (MEK) to ERK. MEK also is known as MKK and MAPKK. It exists as two isoforms, MEK1 and MEK2, which have 79% sequence identity, and each has a similar ability to phosphorylate ERK1 and ERK2. MEK1 has 392 amino acid residues and is regulated by activating phosphorylations at Ser217 and Ser221.[2] Compounds that affect MEK may act by prevention of activation (PoA), where binding to the nonactivated enzyme interferes with its phosphorylation by RAF isoforms such as B-RAF, or they may give inhibition of catalysis (IoC), where binding to activated MEK abrogates phosphorylation of substrates such as ERK. Several publications (e.g., refs *6–9*) involve following catalysis by a nonphosphorylated MEK1, which contains mutations such as Ser217Glu and Ser221Asp designed to mimic the activating phosphorylations. A commonly used construct also has residues 31–50 deleted and is known as ΔN3 (*10*). Compounds often are characterized by measuring IC_{50} at a single concentration of ATP, which does not allow identification of the mechanism of inhibition. MEK inhibitors come from diverse structural types (*6, 7*), many of which are ATP-competitive, although some are not; an early example is a butadiene, U-0126 (*8*), and several noncompetitive inhibitors have some similarity to CI-1040 [PD184352 (*11*)], which is an *N*-alkoxy amide. Crystal structures have been published for analogues of CI-1040 bound to complexes containing MEK and ATP (*12*). Several MEK inhibitors are in clinical trials as agents to treat

* Author for correspondence. E-mail: walter.ward@astrazeneca.com. Tel: +44 (0)1625 515998. Fax: +44 (0)1625 230164.

‡ Present address: BIAcore Inc., Part of GE Healthcare, 800 Centennial Ave., Piscataway, NJ 08854.

[1] Abbreviations: EDTA, ethylenediaminetetraacetic acid; *h*, Hill coefficient; $K_{0.5}$, concentration giving half-maximal rate for a substrate (MEK1) that follows cooperative kinetics; IC_{50}, concentration giving 50% inhibition; IoC, inhibition of catalysis; ISA, inhibition in solution assay; ITC, isothermal titration calorimetry; K_i, inhibition constant for pure noncompetitive inhibition; K_{is}, inhibition constant when substrate (ATP) ≪ K_m; K_{ii}, inhibition constant when substrate (ATP) ≫ K_m; K_{mi}, midpoint concentration for ATP dependence of IC_{50}; MAP, mitogen-activated protein; PoA, prevention of activation.

[2] The residue numbering from Swiss-Prot (see http://www.expasy.org/sprot) is used. Some publications use numbers that are one higher.

10.1021/bi701811x CCC: $40.75
Published on Web 04/05/2008

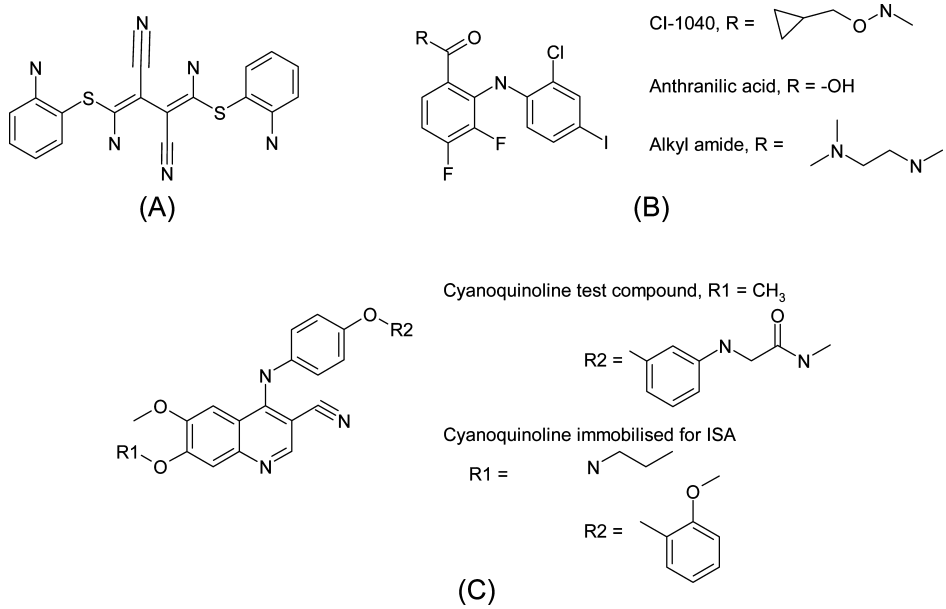

FIGURE 1: Chemical structures of protein kinase inhibitors: (A) U-0126, (B) CI-1040 and analogues, and (C) cyanoquinoline test compound and different cyanoquinolines immobilized for MEK1 inhibition in solution assays. In CI-1040 and the alkyl amide, the R group is attached to give an amide linkage to the core structure. In (C), R2 is attached through an ether linkage and R1 gives a free primary amine on a propoxyl linker for the ISA compound.

cancer. These include ARRY-142886 (AZD6244) and PD0325901 (*7*).

We now report mechanisms deduced from varying the concentration of ATP, in both PoA and IoC, for five MEK inhibitors: U-0126, CI-1040, two CI-1040 analogues (an anthranilic acid and an *N*-alkyl amide), and a cyanoquinoline. These studies used MEK, which is not mutated at the phosphorylation sites, and new insight is gained by linking these kinetic mechanism data with K_d values measured in the presence and absence of ATP. The potency ranking of the compounds changes according to the concentration of ATP and assay format. Potency against nonactivated MEK in PoA resembles that previously reported for constitutively active mutants in IoC. These observations have implications for the identification and evaluation of inhibitors that target MEK and highlight potential considerations for other members of the protein kinase family.

EXPERIMENTAL PROCEDURES

Materials. Full-length, purified, His-tagged B-RAF and ERK2 were from The Division of Signal Transduction Therapy, University of Dundee. Gly-Ser-Ser-MEK1(42–386) was obtained as described in the Supporting Information. Compared to full-length MEK1, this construct gives higher levels of expression, lower (undetectable) autophosphorylation, and lower background in binding assays. Kinetic parameter values change by less than 4-fold when this construct replaces full-length MEK1 as a substrate for B-RAF (see Supporting Information). Protein kinase inhibitors were synthesized in AstraZeneca using procedures described elsewhere for U-0126 (*8*), CI-1040 (*13*), the anthranilic acid (*13*), the *N*-alkyl amide (Supporting Information), the two cyanoquinolines (*14, 15*), and the ureidoquinazoline (*16*). Each compound was at least 80% pure when analyzed by HPLC and NMR.

Inhibition in Solution Assays (ISAs). These were carried out on a BIAcore S51 instrument. An inhibitor was immobilized onto a CM-5 sensor chip using standard amine coupling procedures. For MEK1, it was a cyanoquinoline (Figure 1), and for B-RAF it was the ureidoquinazoline used by Sullivan et al. (*17*). The test compound competes for kinase binding to the immobilized inhibitor, resulting in a signal proportional to the free protein concentration. The chip was calibrated using a report point of 50 s. ISAs were carried out with a flow rate of 30 μL/min in 40 mM *N*-(2-hydroxyethyl)piperazine-*N*′-2-ethanesulfonic acid, pH 7.4, containing 0.2 M NaCl, 5 mM dithiothreitol, 10 mM $MgCl_2$, and 1% dimethyl sulfoxide. Kinases were used at around 200 nM. Surface regeneration between each injection was carried out with 0.5% sodium dodecyl sulfate for 30 s. Dose–response data were analyzed by nonlinear regression with GraFit (Erithacus Software Ltd.) to estimate K_d values by a standard dose–response equation (eq 1) if $K_d \gg$ [MEK1], or a dose–response equation that took into account tight binding of the inhibitor to the protein (eq 2) if K_d was not $\gg$ [MEK1].

$$RU = \frac{RU_{max}}{1 + [I]/K_d} + b \quad (1)$$

$$RU = \left(\frac{RU_{max}}{2}\right)\left[\left(1 - \frac{K_d}{[MEK1]} - \frac{[I]}{[MEK1]}\right) + \sqrt{\left(\frac{K_d}{[MEK1]} + \frac{[I]}{[MEK1]} - 1\right)^2 + \frac{4K_d}{[MEK1]}}\right] + b \quad (2)$$

RU is the signal (response units), RU_{max} is that with no inhibitor, [MEK1] is the concentration of binding sites, and b is background signal. The selection between eqs 1 and 2, with or without the b term, was assisted by an F-test (*18*). All reported values are geometric means from at least three replicate measurements.

Enzyme Assays. Reactions were carried out in a final volume of 25 μL in the same buffer as that used for ISA. Accumulation of product was linear with enzyme concentra-

tion and time. For the B-RAF-dependent phosphorylation of MEK1, final concentrations were 0.02 nM B-RAF, 0.2 μM nonactivated MEK1, 0.625−160 μM ATP, and inhibitor in 1% (v/v) dimethyl sulfoxide. For the MEK1-dependent phosphorylation of ERK2, final concentrations were 10 nM activated MEK1, 0.25 μM ERK2, 12.5−3200 μM ATP, and inhibitor in 1% (v/v) dimethyl sulfoxide. Reactions were stopped after 90 min by addition of 75 μL of 66.6 mM EDTA. A background signal where EDTA was added before ATP was subtracted from each measured rate. The stopped reaction (40 μL) was transferred to a black, high-binding plate (Greiner) and placed at 4 °C overnight to allow binding. ELISA detection of the product was performed as follows. First, plates were flushed three times with washing buffer [100 mM tris(hydroxymethyl)aminomethane hydrochloride, pH 7.5, 154 mM NaCl], containing 0.1% bovine serum albumin and 0.05% Tween 20, and then incubated for 90 min with anti-phospho MEK1 or anti-phospho ERK2 (both from Cell Signaling Technology, Inc.). Next, plates were rinsed three times with washing buffer and then incubated for 90 min with horseradish peroxidase-linked anti-rabbit antibody for phospho-MEK1 (Cell Signaling Technology, Inc.) or horseradish peroxidase-linked anti-mouse antibody for phospho-ERK2 (Sigma). Plates were washed three times prior to incubation with QuantaBlu fluorogenic peroxidase substrate (Pierce Biotechnology, Inc.), and then the fluorescence was measured on a Tecan Sapphire plate reader with 325 nm excitation and 420 nm emission.

Mechanism of Inhibition. This was determined by using GraFit for nonlinear fitting to identify the most suitable rate equation as previously described (*17, 18*). In the absence of inhibitor, B-RAF-dependent phosphorylation of MEK1 follows cooperative kinetics

$$v = \frac{V_{max}[MEK1]_{free}^{h}}{K_{0.5} + [MEK1]_{free}^{h}} \quad (3)$$

where h is the Hill coefficient and $K_{0.5}$ is the free MEK1 concentration giving $v = V_{max}/2$. PoA data were analyzed using equations where inhibitors act by association with substrate (MEK1) and prevent it from binding to enzyme (B-RAF) (see Results and Discussion). The concentration of inhibitor was varied at each of several fixed concentrations of ATP. Equation 3 was fitted to the observed rate, using the remaining concentration of free MEK1, which was estimated using the relationship (*19*)

$$[MEK1]_{free} = \frac{\sqrt{([I] - [MEK1] + IC_{50})^2 + 4IC_{50}[MEK1]} - ([I] - [MEK1] + IC_{50})}{2} \quad (4)$$

where [I] and [MEK1] are the total concentrations added to the assay. This allowed estimation of the IC_{50} and V_{max} at each concentration of ATP. $K_{0.5}$ and h were held constant at the values measured in the absence of inhibitor, because [MEK1] was not varied in the presence of inhibitor. The variation between replicates was larger at higher values of IC_{50}; accordingly, geometric means of these IC_{50} values were used when subsequently fitting relationships for competitive, uncompetitive, and mixed noncompetitive inhibition (*20*), respectively

$$IC_{50} = \frac{K_{is}([ATP] + K_{mi})}{K_{mi}} \quad (5)$$

$$IC_{50} = \frac{K_{ii}([ATP] + K_{mi})}{[ATP]} \quad (6)$$

$$IC_{50} = \frac{K_{is}K_{ii}([ATP] + K_{mi})}{K_{is}[ATP] + K_{ii}K_{mi}} \quad (7)$$

where K_{mi} is the midpoint concentration for the ATP dependence of IC_{50}, which could reflect binding of ATP to MEK or B-RAF. The inhibition constants extrapolating to zero and saturating ATP are respectively K_{is} and K_{ii}. The magnitudes of K_{mi}, K_{is}, and K_{ii} were allowed to vary in order to estimate the best-fit parameter values. For pure noncompetitive inhibition, IC_{50} is independent of ATP concentration and so equals K_i. The mechanism of inhibition in PoA was determined by identifying which relationship (eq 5, 6, or 7 or $IC_{50} = K_i$) best described the ATP dependence of IC_{50}. Global (multivariate) regression was not used, because the equations (eqs 8−11) gave poor quality of fit. This may be because they did not allow for depletion of free substrate and because the ATP dependence may be complicated, reflecting binding to both MEK1 and B-RAF.

Global regression was used for IoC data, where inhibitor and ATP were varied in the same fit for the equations

$$v = \frac{V_{max}[ATP]}{K_m(1 + [I]/K_{is}) + [ATP]} \quad (8)$$

$$v = \frac{V_{max}[ATP]}{K_m + [ATP](1 + [I]/K_{ii})} \quad (9)$$

$$v = \frac{V_{max}[ATP]}{K_m(1 + [I]/K_i) + [ATP](1 + [I]/K_i)} \quad (10)$$

$$v = \frac{V_{max}[ATP]}{K_m(1 + [I]/K_{is}) + [ATP](1 + [I]/K_{ii})} \quad (11)$$

which respectively describe competitive, uncompetitive, pure noncompetitive, and mixed noncompetitive inhibition (*20*).

Isothermal Titration Calorimetry (ITC). This was carried out using a VP-ITC instrument (MicroCal, Inc., Northampton, MA) as previously described (*17*) at 25 °C in the same buffer as that used for ISA except 5 mM tris(2-carboxyethyl)phosphine hydrochloride replaced 5 mM dithiothreitol. The concentration of MEK1 was determined using a stoichiometric binding inhibitor by ISA and was used at 3.5–15 μM. Compounds were diluted from a 100% dimethyl sulfoxide stock solution, and the final dimethyl sulfoxide concentration was adjusted to 1%. Final protein and compound solutions were degassed for 7 min. Curves were fitted by nonlinear regression using a one-site binding model provided by MicroCal Origin software (version 5.0). Reported values of $\Delta H°$, $\Delta G°$, and K_d are the means of at least two titrations, and $T\Delta S°$ was estimated as ($\Delta H° - \Delta G°$).

RESULTS

Characteristics of Uninhibited Kinases. Compounds have been investigated with respect to their effects on the phosphorylation of nonactivated MEK1 by B-RAF and the phosphorylation of ERK2 by activated MEK1. The design of these experiments and interpretation of the results were facilitated by first characterizing each of these processes in the absence of inhibitors. The kinetic parameters for B-RAF-

Table 1: Kinetic Characteristics for Phosphorylation of MEK1 by B-RAF[a]

parameter	value
K_d(ATP) from activated B-RAF	$7.8 \pm 2.2\ \mu$M
K_d(ATP) from nonactivated MEK1	$2.7 \pm 0.1\ \mu$M
K_m(ATP) at 0.15 μM MEK1	$15 \pm 8\ \mu$M
K_m(ATP) at 0.6 μM MEK1	$13 \pm 2\ \mu$M
$K_{0.5}$(MEK1) at 10 μM ATP	$0.22 \pm 0.06\ \mu$M[b]
Hill coefficient for MEK1 at 10 μM ATP	2.0 ± 0.4[b]
$K_{0.5}$(MEK1) at 100 μM ATP	$0.23 \pm 0.05\ \mu$M[b]
Hill coefficient for MEK1 at 100 μM ATP	2.5 ± 0.3[b]
k_{cat}	$0.66 \pm 0.30\ s^{-1}$
$k_{cat}/K_{0.5}$(MEK1)	$3.0 \times 10^6\ s^{-1}\ M^{-1}$

[a] K_d values were estimated using ISA. [b] Followed cooperative kinetics. $K_{0.5}$ is the concentration giving 50% maximal rate. k_{cat} is the catalytic rate constant (mole of product per mole of enzyme per second). Each measurement was made in duplicate in at least two experiments.

dependent phosphorylation of MEK1 are shown in Table 1. The midpoint ATP concentration is similar for binding to activated B-RAF and binding to nonactivated MEK1 and for the kinetics of phosphorylation. Prior to phosphorylation by B-RAF, MEK1 has no detectable catalytic activity (at least 350000-fold lower than activated MEK1). There is no significant shift in K_m for ATP when the concentration of MEK1 is changed from 0.15 to 0.6 μM (Figure 2A, Table 1). MEK1 dependence exhibits a Hill coefficient around 2.0−2.5 showing positive cooperativity (Figure 2B), perhaps because phosphorylation at one site promotes phosphorylation at the other, which is four residues away. Again the concentration of one substrate (ATP = 10 or 100 μM) has little effect on the midpoint concentration, $K_{0.5}$, of the other (Table 1).

Activated MEK1 has a K_m(ATP) of 190 μM at 0.5 μM ERK2 in the current work (Table 2). This is only 3.5-fold lower than the reported K_d(ATP) of 700 μM for nonactivated ERK2 (*21*), so that it is difficult to ascertain whether the rate in IoC is affected by association of ATP with ERK2 or MEK1. The measured K_m for ERK2 is over 3 μM at 200 μM ATP. The K_m(ATP) for activated MEK1 is 71-fold higher than the K_d from the nonactivated form. This could reflect decreased affinity after activation or the effects of additional kinetic steps when there is catalysis rather than only binding. Nonphosphorylated MEK1 and phosphorylated MEK1 exhibit K_d values around 2 μM for ATP analogues (*22*), which are similar to the $K_d = 2.7\ \mu$M for ATP binding nonactivated MEK1.

Prevention of Activation. In order to characterize effects on PoA, compounds were evaluated in assays, which followed the B-RAF-dependent phosphorylation of nonactivated MEK1. Data were analyzed using eqs 3 and 4, where the inhibitor acts by binding MEK1 rather than B-RAF. The evidence for this mode of action is considered in the Discussion. All inhibitor dose–response studies were performed at 0.2 μM MEK1, so the parameters $K_{0.5}$ and h were held constant at the values obtained in the absence of inhibitor, 0.23 μM and 2.0, respectively (Table 1). A representative data set for U-0126 at 40 μM ATP is shown to give an acceptable quality of fit (Figure 3). During this fit, [MEK1] was allowed to vary, because depletion of the low inhibitor concentrations by binding to this protein allowed calculation of a best-fit value of $0.19 \pm 0.02\ \mu$M, which agreed with the added concentration (determined by ISA and ITC) of 0.20 μM. Most data sets gave higher IC_{50} values, so that estimated [MEK1] lacked precision because depletion of inhibitor was less significant. Accordingly, the value of [MEK1] was held constant at 0.20 μM to generate the results reported in Figure 4.

Inhibition of Catalysis. In order to characterize the effects on IoC, compounds were tested in assays, which followed the phosphorylation of ERK2 by activated MEK1. Data were analyzed using rate eqs 8−11, where the inhibitor binds to activated MEK1. The evidence relating to this mechanism is considered in the Discussion. Representative IoC results are shown in Figure 5, where U-0126 follows pure noncompetitive kinetics (eq 10) that reduce V_{max} and do not change K_m. Different ATP concentrations were used in PoA and IoC (Figure 4), because its affinity changes from $K_d = 2.7\ \mu$M to $K_m = 190\ \mu$M, following the activation of MEK1.

Characteristics of Compounds. Compounds were evaluated in PoA, IoC, and binding assays (ISA and ITC). The aim was to provide complementary data from orthogonal assays in order to obtain an integrated insight into the mode of action. The assigned mechanisms of inhibition, together with calculated inhibition constants, are given in Table 4. The IoC data are less noisy than those from PoA (Figure 4), perhaps because the consequences of binding to an enzyme (in IoC) are amplified by multiple catalytic events, unlike the consequences of binding to a substrate (in PoA). There are some systematic deviations in the fits to IC_{50} against ATP concentration, suggesting that the assigned mechanisms may be an approximation, rather than a precise description of the system. The deviations could reflect interaction between substrates or cooperative effects.

The IC_{50} values represent apparent inhibition constants under the conditions of the assay. There is no evidence for these IC_{50}s being perturbed by nonspecific inhibition (see ref *23*) or slow binding (where potency changes over time).

(1) U-0126. In PoA, inhibition is assigned as mixed noncompetitive (eq 7), $K_{is} = 0.48\ \mu$M and $K_{ii} = 0.10\ \mu$M, because potency changes up to 5-fold with ATP concentration (Figure 4). These characteristics show similarities with the affinity of binding to nonactivated MEK1, which is little affected by the degree of saturation with ATP (Tables 3 and 5), with ITC giving midpoints, which are close to the inhibition constants from PoA. The affinity measured by ISA is higher than that in ITC (see below). The IC_{50} in IoC is independent of ATP concentration, following pure noncompetitive kinetics (eq 10), $K_i = 1.3\ \mu$M (Figure 4). A decrease in potency has been reported on moving from PoA using C-RAF to IoC using ERK2 [IC_{50}s of 0.3 and 20 μM (*24*)]. The higher IoC IC_{50} may reflect reported chemical instability of U-0126 (*25*).

(2) CI-1040. This compound tends toward giving uncompetitive inhibition in PoA (eq 6), $K_{ii} = 0.31\ \mu$M, indicating that inhibition when ATP is below K_{mi} is much weaker than when it is saturating (Figure 4). This is similar to the midpoint for binding to nonactivated MEK1 in ISA decreasing 22-fold to 0.074 μM following addition of 5 μM ATP (Table 3). The observation of CI-1040 preventing activation by B-RAF is in agreement with a previous report of it preventing C-RAF-dependent activation (*24*). Inhibition is not affected by ATP concentration in IoC, because it is pure noncompetitive (eq 10), with $K_i = 0.19\ \mu$M (Figure 4).

(3) Anthranilic Acid. The IC_{50} of this CI-1040 analogue in PoA changes little with ATP concentration, approximating

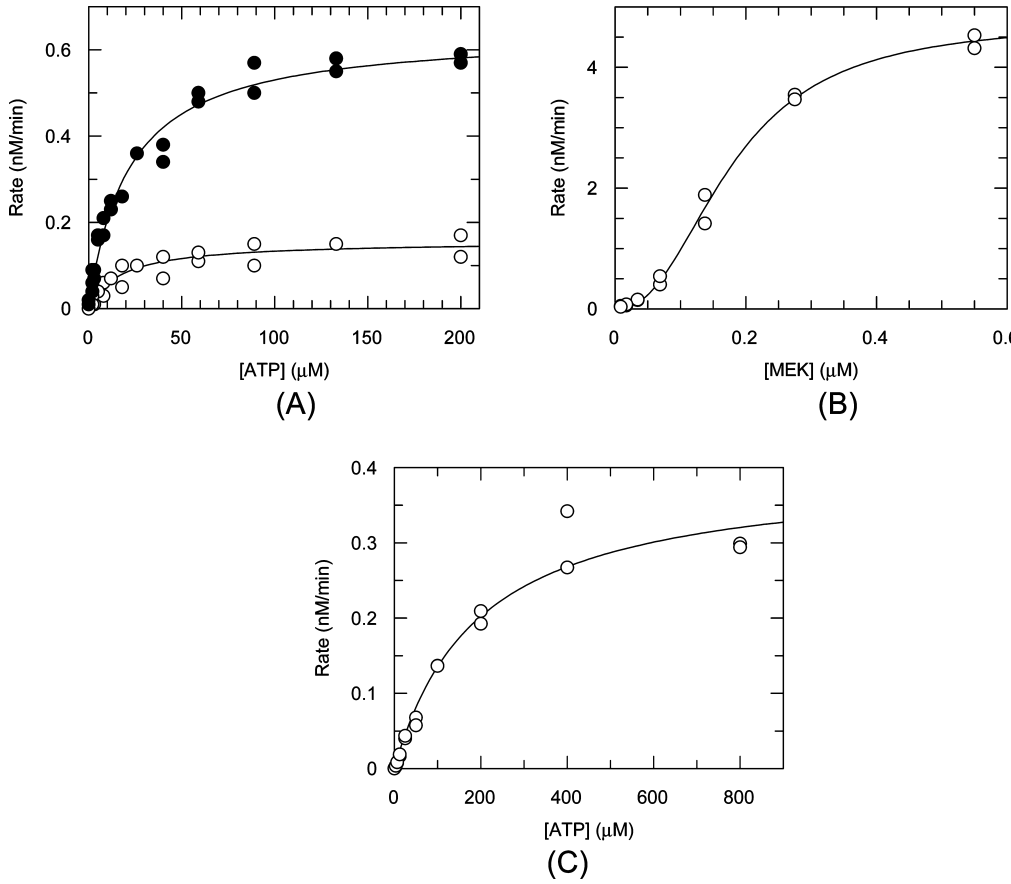

FIGURE 2: ATP and substrate dependence for phosphorylation of MEK1 and ERK2. (A) ATP dependence for phosphorylation by 0.01 nM B-RAF at (○) 0.15 μM and (●) 0.6 μM MEK1. The lines are drawn using the best-fit values for the Michaelis–Menten equation, which are $V_{max} = 0.16 \pm 0.01$ nM/min, $K_m = 17 \pm 3$ μM at 0.15 μM MEK1 and $V_{max} = 0.64 \pm 0.02$ nM/min, $K_m = 21 \pm 2$ μM at 0.6 μM MEK1. (B) MEK1 dependence for phosphorylation by 0.1 nM B-RAF at 10 μM ATP. The line is drawn using the best-fit values for the Hill equation (eq 3), which are $V_{max} = 4.8 \pm 0.2$ nM/min, $K_{0.5} = 0.18 \pm 0.01$ μM, and Hill coefficient $= 2.3 \pm 0.2$. (C) ATP dependence for phosphorylation by 5 nM MEK1 at 0.5 μM ERK2. The line is drawn using the best-fit values for the Michaelis–Menten equation, which are $V_{max} = 0.40 \pm 0.03$ nM/min and K_m 190 $\pm$ 30 μM.

Table 2: Kinetic Characteristics for Phosphorylation of ERK2 by MEK1[a]

parameter	value
K_m(ATP) at 0.5 μM ERK2	190 $\pm$ 30 μM
K_m(ERK2) at 0.15 μM ATP	>3 μM
k_{cat}	>0.007 s^{-1}
k_{cat}/K_m(ATP)	>39 s^{-1} M^{-1}

[a] Could not measure rate at sufficiently high concentrations of ERK2 to allow estimation of K_m. k_{cat} is the catalytic rate constant (mole of product per mole of enzyme per second). Each measurement was made in duplicate in at least two experiments.

to pure noncompetitive inhibition, $K_i = 0.45$ μM (Figure 4). This is consistent with the binding to nonactivated MEK1 in ISA and ITC, giving midpoints between 0.11 and 0.40 μM (Tables 3 and 5). In IoC, the mean IC_{50} increases only 1.7-fold on moving from 12.5 to 3200 μM ATP, consistent with pure noncompetitive kinetics (eq 10), $K_i = 1.0$ μM (Figure 4).

(4) Akyl Amide. In PoA, this compound appears to require prior binding of ATP, giving uncompetitive inhibition (eq 6), $K_{ii} = 2.4$ μM (Figure 4). This is similar to the binding affinity for nonactivated MEK1, where the midpoint decreases over 17-fold to 2.9 μM following addition of 5 μM ATP (Table 3), and is 0.66 μM at 100 μM ATP (Table 5). Conversely, in IoC, the alkyl amide is not affected by the

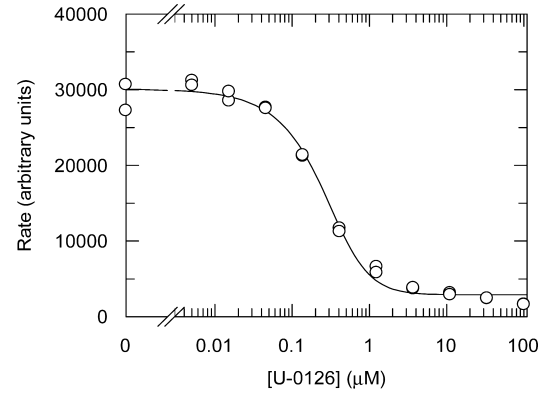

FIGURE 3: Dose–response curve for U-0126 inhibiting phosphorylation of MEK1 by B-RAF. Concentrations were 0.2 μM MEK1, 0.02 nM B-RAF, and 40 μM ATP. The line is drawn using the best-fit values for inhibitor binding to substrate (eqs 3 and 4), $IC_{50} = 0.28 \pm 0.04$ μM, [MEK1] $= 0.19 \pm 0.02$ μM, $V_{max} = 66000 \pm 6000$ units, and background rate $= 2900 \pm 400$ units. The values of $K_{0.5}$ and h were held constant at 0.23 μM and 2.0, respectively.

degree of saturation with ATP, exhibiting pure noncompetitive kinetics (eq 10), $K_i = 2.7$ μM (Figure 4).

(5) Cyanoquinoline. The IC_{50} values in PoA are independent of ATP concentration, consistent with pure noncompetitive inhibition, $K_i = 1.29$ μM (Figure 4). This compound appears to have tighter, stoichiometric binding to nonacti-

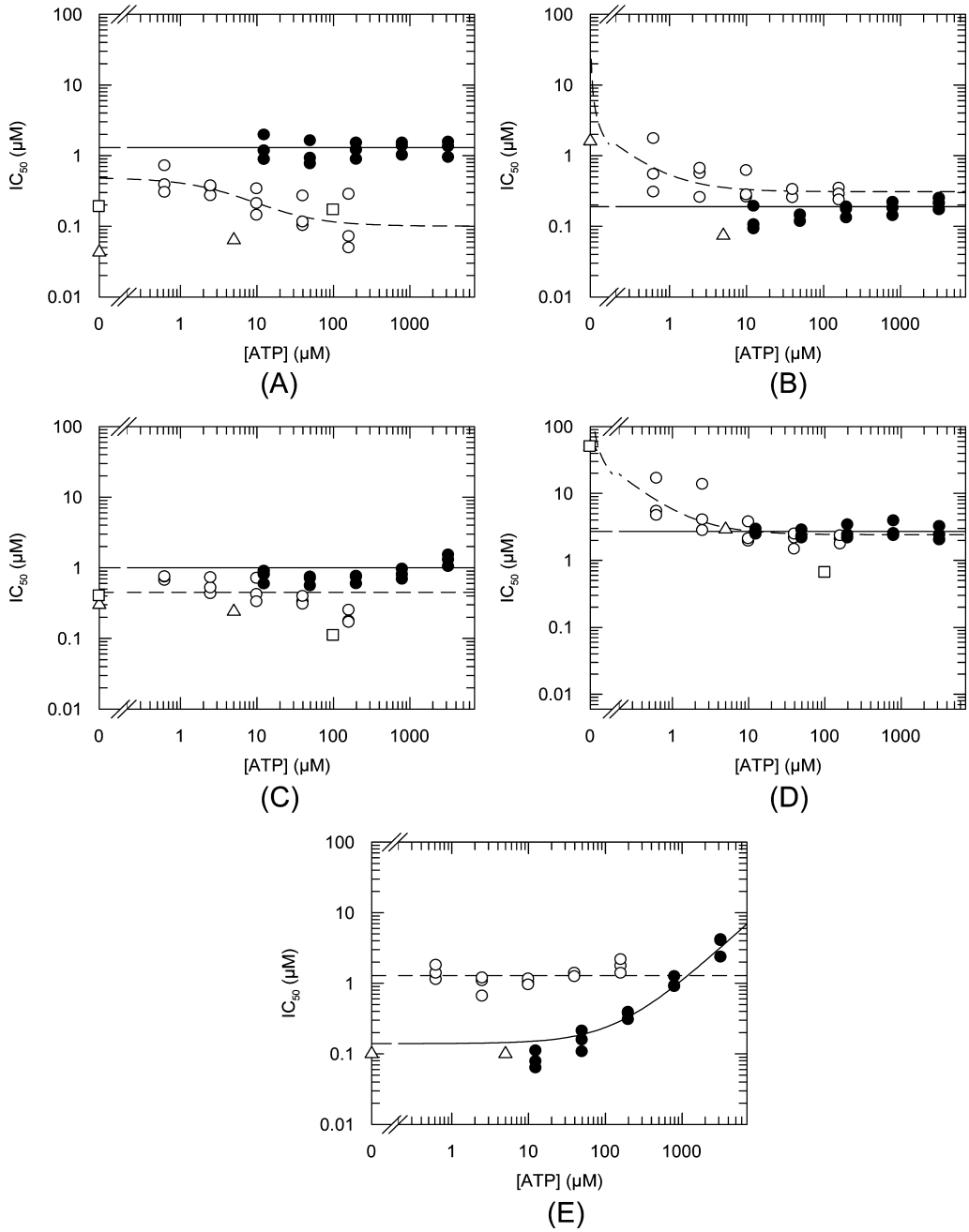

FIGURE 4: ATP dependence of IC_{50}: (○) B-RAF-dependent phosphorylation of MEK1 (PoA); (●) MEK1-dependent phosphorylation of ERK2 (IoC). Panels: (A) U-0126, (B) CI-1040, (C) anthranilic acid, (D) alkyl amide, and (E) cyanoquinoline. IoC IC_{50}s were estimated by fitting to eq 1, modified to use rates in place of RUs and IC_{50} in place of K_d. PoA IC_{50}s were estimated by fitting to eqs 3 and 4, with the values of $K_{0.5}$ and h held constant at 0.23 μM and 2.0, respectively. Lines are drawn using the best-fit parameter values (Table 4): dashed lines for PoA and solid lines for IoC. The mean K_d values from ISA and ITC are shown as (△) and (□), respectively.

Table 3: K_d Values for Nonactivated MEK1 from ISA[a]

inhibitor	K_d (μM)	app K_d with 5 μM ATP (μM)
U-0126	0.043 ± 0.031	0.064 ± 0.040
CI-1040	1.6 ± 1.2	0.074 ± 0.038
anthranilic acid	0.30 ± 0.16	0.24 ± 0.11
alkyl amide	>50	2.9 ± 2.4
cyanoquinoline	<0.1	<0.1

[a] Each compound has a K_d > 10 μM for activated B-RAF. Each measurement was made in duplicate in at least three experiments.

vated MEK1 in the absence of B-RAF, because ISA gives a K_d <0.1 μM in the presence or absence of 5 μM ATP (Table 3). K_d could not be measured in ITC, due to insufficient heat change following addition of the compound. In IoC, the cyanoquinoline follows ATP-competitive kinetics (eq 8), K_{is} = 0.14 μM (Figure 4).

Thermodynamics of Binding. ITC was used to measure affinity, enthalpy, entropy, and stoichiometry of binding, whereas ISA yields only K_d values. Unlike ISA, ITC is a direct binding assay that does not require displacement of another inhibitor. The techniques are complementary in that ISA allows characterization of binding of the cyanoquinoline, which is not detected in ITC.

In ITC, ATP, U-0126, the anthranilic acid, and the alkyl amide each exhibit a stoichiometry close to 1, which is consistent with specific binding to nonactivated MEK1 (Table 5). For ATP or the anthranilic acid, the K_d values from ITC are within 1.6-fold of those from ISA (Tables 1 and 3).

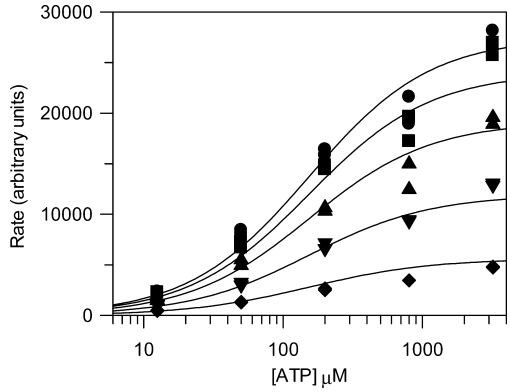

FIGURE 5: Inhibition of MEK1-dependent phosphorylation of ERK2 by U-0126. Rates were measured at 10 nM MEK1 and 0.25 μM ERK2. The lines are drawn using the best-fit parameter values from global fitting of eq 10, which are $V_{max} = 28000 \pm 1000$ units, $K_m = 160 \pm 10$ μM, and $K_i = 0.95 \pm 0.07$ μM. Concentrations of U-0126 were (●) 0 μM, (■) 0.14 μM, (▲) 0.41 μM, (▼) 1.2 μM, and (◆) 3.7 μM. For clarity, data at six further concentrations are not shown.

U-0126, however, has a 4.4-fold higher K_d in ITC. The observed stoichiometry suggests that this is not due to the reported instability of U-0126 (*25*). Binding of U-0126 may be sensitive to the different concentrations of MEK1 in ISA and ITC. The observed heat change is similar to the heat of dilution when the alkyl amide or cyanoquinoline is titrated into free MEK1. The alkyl amide result is consistent with ISA, which does not detect binding to free MEK1 (Table 3). In the presence of 100 μM ATP, the alkyl amide has a midpoint of 0.66 μM, suggesting that the free enzyme data could be due to K_d being over 50 μM. The cyanoquinoline again gives only the heat of dilution when titrated into MEK1 in the presence of 100 μM ATP. Given that ISA indicates binding (Table 3), it could be that the association of this compound with MEK1 gives a heat change that is too small to detect. Insight into the mechanism is obtained from measurements at 100 μM ATP, which is approaching saturation (Table 5). The ATP dependence in binding is similar to that in PoA for U-0126, the anthranilic acid (both noncompetitive), and the alkyl amide (which is uncompetitive; Table 4).

DISCUSSION

Comparison with Previous Studies. Nonactivated wild-type MEK1 has been reported to have $V_{max} = 0.001$ s^{-1}, K_m ATP = 308 μM, and K_m[ERK2(Lys52Ala)] = 19 μM (*10*), which is similar to the lack of detectable catalysis by nonactivated MEK1 in the current work. Following phosphorylation by v-Mos, these parameters change respectively to 0.024 s^{-1}, 3.5 μM, and 0.34 μM. The differences relative to Table 2 could reflect changes in the MEK or ERK constructs, following specific phospho transfer (current work) rather than total phospho transfer (*10*), or changes in other assay conditions.

Several studies have used constitutively active MEK enzyme that has been mutated to mimic phosphorylation. Such a model has not been used in the current work, where the nonactivated MEK contained Ser217 and Ser221 or the activated enzyme was phosphorylated at these positions. Limited data suggest that constitutively active mutant MEK resembles the nonactivated enzyme. U-0126 follows ATP-noncompetitive kinetics in both PoA ($K_{is} = 0.48$, $K_{ii} = 0.10$ μM) and IoC (K_i 1.3 μM) (Table 4). Similar inhibition constants ($K_i = 0.041$ μM -0.109 μM) in IoC by constitutively active mutant MEK1 and weaker inhibition in IoC by phosphorylated wild-type MEK1 have been reported for U-0126 (*8*). CI-1040 has an apparent $K_d = 0.074$ μM from nonactivated MEK1 in the presence of 5 μM ATP (Table 3) and a $K_i = 0.19$ μM in IoC (Table 4). This compound has an $IC_{50} = 0.017$ μM against double mutant MEK (*7*). The mutant MEK has K_m(ATP) = 5.6 μM (*26*), which is similar to the K_d from nonactivated MEK1 of 1.9−2.7 μM in the current work.

Molecular Mechanism of Inhibition. Several observations suggest that each of these compounds may act by binding to MEK1, rather than B-RAF, in order to give PoA. First, each compound inhibits catalysis by activated MEK1 in the absence of B-RAF. Also, none of the compounds compete with the immobilized ureidoquinazoline binding to activated B-RAF (Table 3). Conversely, they have mean PoA IC_{50}s of 0.33−5.4 μM at 2.5 μM ATP (Figure 4) and apparent K_d values of 0.064−2.9 μM when binding to nonactivated MEK1 at 5 μM ATP (Table 3). The compounds do, however, vary in terms of the relationship between potency in PoA (Table 4) and affinity for nonactivated MEK1 (Tables 3 and 5).

The evidence above also suggests that they may bind to activated MEK1 in order to inhibit phosphorylation of ERK2, although it is possible that affinity and activity change according to the activation state and molecular partners for MEK1. Three of the compounds (CI-1040, the anthranilic acid, and the alkyl amide) have potencies in IoC where MEK1 is the enzyme, which are similar to those in PoA where MEK1 is the substrate and ERK2 is absent (Table 4). Furthermore, four compounds (U-0126, CI-1040, and its two analogues) exhibit mean IC_{50}s below 3 μM when MEK1 phosphorylates ERK2 (Figure 4), and when present at 10 μM, each gives less than 25% inhibition when MEK1 is absent during ERK2-dependent phosphorylation of myelin basic protein (not shown).

The equations (eqs 3 and 4) used to analyze PoA data are based on the hypothesis that the compound competes with B-RAF for binding to MEK1 (Figure 6). X-ray crystallography shows that association with PD318088 leads MEK1 to adopt an inactive conformation (*12*). This compound is similar to CI-1040, the anthranilic acid, and the alkyl amide, so they are likely to induce a similar conformation of MEK1. These conformation changes may prevent binding to B-RAF. This model is consistent with our preliminary data for CI-1040, which indicate an increase in PoA IC_{50} when the concentration of MEK1 is increased (not shown). In similar PoA assays, a pyrazolourea, which induces a different conformation change in p38α, appears to follow substrate-competitive kinetics when inhibiting MKK6-dependent phosphorylation of p38α (*17*).

Hypothetical mechanisms for PoA may be suggested for CI-1040, the anthranilic acid, and the alkyl amide (Figure 6). Binding of PoA inhibitor to MEK1 is proposed to block association with B-RAF. The value of K_{is} may reflect binding to free MEK1, extrapolating to zero ATP, whereas K_{ii} could relate to binding to the MEK·ATP complex at saturating ATP, where ATP dependence (K_{mi} in eqs 5−7) may be the K_d for ATP binding to MEK1. The ATP-noncompetitive

Table 4: Kinetic Characteristics of MEK Inhibitors[a]

	U-0126	CI-1040	anthranilic acid	alkyl amide	cyanoquinoline
			B-RAF-Dependent Activation of MEK1 (PoA)		
K_{is} (μM)	0.48 ± 0.02	ND	ND	ND	ND
K_{ii} (μM)	0.10 ± 0.01	0.31 ± 0.02	ND	2.4 ± 0.6	ND
K_i (μM)	ND	ND	0.45 ± 0.09	ND	1.29 ± 0.14
mechanism	mixed	UC	PNC	UC	PNC
			MEK1-Dependent Phosphorylation of ERK2 (IoC)		
K_{is} (μM)	ND	ND	ND	ND	0.14 ± 0.04
K_i (μM)	1.3 ± 0.3	0.19 ± 0.04	1.0 ± 0.2	2.7 ± 0.7	ND
mechanism	PNC	PNC	PNC	PNC	C
IoC/PoA[b]	13	0.61	2.2	1.1	0.11

[a] PoA, prevention of activation; IoC, inhibition of catalysis. K_{is} and K_{ii} are respectively the inhibition constants when [ATP] is at negligible or saturating concentrations. C, competitive; MNC, mixed noncompetitive; PNC, pure noncompetitive (K_i reported, which is $\approx K_{is} \approx K_{ii}$); UC, uncompetitive. ND, not determined. [b] Ratio of inhibition constants. PoA values are from fitting the ATP dependence of IC_{50} (eq 5 to eq 7); IoC values are from global fitting (eq 8 to eq 11); see Experimental Procedures. Values for K_{mi}(ATP) in PoA were 20 ± 5 μM for U-0126, 0.74 ± 0.15 μM for CI-1040, and 1.4 ± 0.6 μM for alkyl amide. K_m(ATP) was 140 ± 40 μM for cyanoquinoline in IoC. Each study involved duplicate measurements and was repeated three times.

Table 5: Thermodynamics for Binding to Nonactivated MEK1[a]

	±100 μM ATP	K_d (μM)	$\Delta G°$ (kcal/mol)	$\Delta H°$ (kcal/mol)	$T\Delta S°$ (kcal/mol)	n
ATP		1.9 ± 0.4	−7.8 ± 0.1	−15.6 ± 2.0	−7.8 ± 2.1	0.95 ± 0.03
U-0126	−	0.19 ± 0.01	−9.2 ± 0.1	−17.4 ± 0.4	−8.2 ± 0.2	0.91 ± 0.29
	+	0.17 ± 0.01	−9.3 ± 0.1	−9.5 ± 1.1	−0.2 ± 0.2	1.1 ± 0.1
anthranilic acid	−	0.40 ± 0.18	−8.7 ± 0.3	−12.0 ± 1.0	−3.3 ± 1.2	1.1 ± 0.1
	+	0.11 ± 0.03	−9.5 ± 0.2	−8.1 ± 1.4	1.4 ± 1.6	1.2 ± 0.4
alkyl amide	−	>50[b]				
	+	0.66 ± 0.15	−8.4 ± 0.1	−2.3 ± 0.1	6.1 ± 0.2	1.3 ± 0.1

[a] Each measurement was made between two and five times. [b] Binding not detected by ITC; value from ISA.

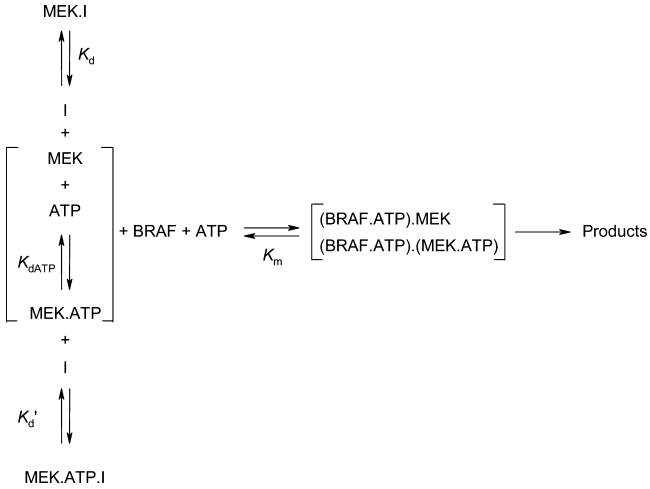

FIGURE 6: Possible kinetic scheme for prevention of activation. The different complexes within brackets cannot be distinguished in these experiments. The parentheses indicate which kinase is bound by the ligand. K_d and K_d' are respectively the dissociation constants for I from the MEK•I complex in the absence of ATP and the MEK•ATP•I complex at saturating ATP. K_{dATP} is the dissociation constant of ATP from MEK. K_m is that for ATP when B-RAF phosphorylates MEK.

kinetics for the anthranilic acid are consistent with it binding MEK1 and the MEK1•ATP complex with similar affinities (Tables 3 and 5). CI-1040 and the alkyl amide each follow ATP-uncompetitive kinetics, consistent with binding to MEK1 being favored by prior association with ATP (Tables 3 and 5). This hypothesis is consistent with CI-1040 and the alkyl amide giving ATP-dependent IC_{50} values, where the K_{mi}(ATP) values estimated from eq 6 are 0.74 and 1.4 μM, respectively, which are close to the K_d for ATP from nonactivated MEK1 (1.9−2.7 μM, Tables 3 and 5). In the crystal structure of a complex between nonactivated MEK1, ATP, and PD318088, the alkoxy amide side chain of the inhibitor interacts with bound ATP and with Lys96, which forms part of the ATP pocket (*12*). These interactions may contribute to the observed requirement for prior association with ATP when CI-1040 and the alkyl amide bind to nonactivated MEK1. The anthranilic acid lacks this side chain, perhaps explaining why ATP is not required.

The mixed noncompetitive ATP dependence of IC_{50} for U-0126 (eq 7) gives a K_{mi} ATP = 20 μM, which is close to the K_m(ATP) = 14 μM for B-RAF in the absence of inhibitor. It may be that this value is inaccurate, reflecting noise in the data (Figure 4), and U-0126 follows the same pure noncompetitive mechanism as the anthranilic acid. Alternatively, U-0126 could bind to MEK1 in a complex with B-RAF, which has not been detected in this work because MEK1 and inhibitor have not been varied in the same experiment. This mechanism could mean that the IC_{50} values from eqs 3 and 4 are not accurate. For the cyanoquinoline, potency in PoA (K_i = 1.29 μM) is weaker than K_d (<0.1 μM), suggesting that it reduces the affinity of MEK1 for B-RAF, rather than completely preventing binding. The ATP-noncompetitive inhibition by this compound in PoA (Figure 4) was not expected and may reflect a direct or indirect link with the site used by CI-1040. This idea is consistent with the observation that a related immobilized cyanoquinoline competes with each of the compounds for binding to MEK1 (Table 3), despite them having different mechanisms of action. It could be that the cyanoquinoline uses different binding modes, depending upon the MEK1 activation status. Similarly, there is precedent for a compound showing different binding modes for two related kinases: Gleevec

Table 6: Inhibitor Potency in Different Assay Formats[a]

	U-0126	CI-1040	anthranilic acid	alkyl amide	cyanoquinoline
IC_{50} at [ATP] = K_m in IoC (μM)	1.3	0.19	1.0	2.7	0.28
relative IC_{50}	1.0	1.0	1.0	1.0	1.0
K_d for nonactivated MEK1 (μM)	0.043[b]	1.6	0.30	>50	<0.1
relative to IoC IC_{50}	0.033[c]	8.4	0.30	>18	<0.36
IC_{50} at ATP = K_m in PoA (μM)	0.17	0.62	0.45	4.8	1.29
relative to IoC IC_{50}	0.13	3.3	0.45	1.8	4.6
IC_{50} at 2 mM ATP in IoC (μM)	1.3	0.19	1.0	2.7	1.6
relative to IoC IC_{50}	1.0	1.0	1.0	1.0	5.7

[a] K_d values from ISA. [b] K_d from ITC = 0.19 μM. [c] 0.15 for K_d from ITC. IC_{50} values calculated from eqs 5−7 using inhibition constants in Table 4; K_m(ATP) = 14 μM in PoA (Table 2) and 190 μM in IoC (Table 3).

extends from the ATP site into an adjacent "selectivity pocket" on ABL (*27*), whereas it uses only the ATP site on SYK (*28*).

In PoA assays with certain compounds at some concentrations of ATP, there is a small, reproducible residual rate at saturating concentrations of inhibitor (Figure 3). This may represent partial inhibition, which has been reported during inhibition of p38-dependent phosphorylation of MK2a (*29*) and MKK6-dependent phosphorylation of p38 (*17*).

In ITC, U-0126 and the anthranilic acid each exhibit $\Delta G°$ values, which change little on moving from the free enzyme to the enzyme−ATP complex (Table 5). The enthalpies of binding show larger changes, indicating enthalpy–entropy compensation, which is common in biological systems (*30*). There is a lower entropic penalty for binding of either U-0126 or the anthranilic acid to the MEK1·ATP complex, suggesting that prior association with ATP reduces the conformational flexibility of the inhibitor binding site.

The cyanoquinoline shows around 9-fold lower potency in PoA than in IoC, and it has a K_d from nonactivated MEK1 <0.1 μM, which could be similar to the K_{is} = 0.14 μM in IoC by activated MEK1. Phosphorylation on the activation loop is known to cause large conformation changes in several protein kinases, which may explain the different ATP dependencies for this compound in PoA and IoC. The cyanoquinoline is ATP-competitive in IoC, and eq 8 gives an estimate of K_m for ATP = 140 μM, which is similar to that in the absence of inhibitors. ATP-competitive inhibition is expected, given the structural similarity to adenine and precedence of quinolines binding in the purine site of other protein kinases (*4, 31, 32*).

Effects of Assay Format on Potency. Kinase drug discovery often involves ranking of compound potency in assays that follow IoC when ATP is present around its K_m concentration. In terms of IC_{50}, the compounds under investigation rank CI-1040 ≈ cyanoquinoline < anthranilic acid ≈ U-0126 < alkyl amide (Table 6). However, four of the compounds give a K_d for nonactivated MEK1 in ISA, which varies between 30-fold lower and over 18-fold higher than this IoC IC_{50}, with U-0126 becoming the most potent and CI-1040 the least potent. (The K_d for the cyanoquinoline is excluded from this comparison, because its precise value has not been measured.) In PoA at K_m(ATP), U-0126 again is the most potent compound, becoming more potent than CI-1040, the cyanoquinoline, and the anthranilic acid. These shifts in IC_{50} arise because the compounds exhibit different K_i values or ATP dependence in PoA relative to IoC (Table 4). For U-0126, CI-1040, the acid, and the amide, the ATP dependence in binding assays is similar to that in PoA (Figure 4, Tables 3−5). The changes in ATP dependence between compounds lead to the assay format having quite different effects on potency (Table 6):

(1) When the ATP concentration equals K_m, IC_{50} in PoA varies between 4.6-fold higher and 7.7-fold lower than that in IoC.

(2) K_d in an affinity screen against nonactivated MEK1 would be over 8-fold higher than IC_{50} in IoC for CI-1040 and the alkyl amide (Tables 3 and 4). The K_d in ISA is lower than IoC IC_{50} for U-0126 and the anthranilic acid.

(3) The cyanoquinoline is ATP-competitive in IoC; accordingly, its IC_{50} increases over 5-fold on moving the ATP concentration from K_m to physiological (approximately 2 mM). The change is less than 2-fold for the other four compounds (Figure 4, Table 6).

(4) Despite the structural similarities between CI-1040, the anthranilic acid, and the alkyl amide (Figure 1), these three compounds follow different mechanisms in PoA and binding to nonactivated MEK1 (Tables 3−5). Binding of CI-1040 or the alkyl amide is strongly favored by prior association with ATP. A similar effect has been seen for another CI-1040 analogue, PD0325901 (*22*). Conversely, the anthranilic acid has similar affinities in the presence and absence of ATP. CI-1040 and the alkyl amide change mechanism from ATP-uncompetitive in PoA to pure noncompetitive in IoC, possibly reflecting a difference in the MEK phosphorylation state or the change in partner from B-RAF to ERK2.

Affinity screening is increasingly being used to identify compounds of interest in drug discovery. Techniques deployed include X-ray crystallography (*33*), NMR (*34*), thermal stabilization (*35*), mass spectrometry (*36*), or displacement assays (*37*). The measured K_d values (Tables 3 and 5) have implications for the results, which would be obtained from affinity screening against free, nonactivated MEK1. Binding assays could underestimate the biological activity of CI-1040 or the alkyl amide, but not the anthranilic acid. This illustrates the potential value in using affinity screening against a mixture containing the MEK·ATP complex rather than the free enzyme. This principle appears to be widely applicable, because around 30% of drugs require prior binding of another ligand (*38*).

These results highlight aspects of drug discovery applied to MEK:

(1) A single compound gives different IC_{50} values against the same target protein in different assays, which introduces challenges into evaluation of potency and selectivity (*5*). Similarly, three compounds previously have been shown to have quite different potencies against p38α MAP kinase, according to whether the assay follows PoA or IoC (*17*). A biarylbutyranilide is much more potent against p38α when MK2a rather than ATF-2 is used as the substrate (*29*). The current work illustrates that determination of the mechanism of action and measurement of inhibition constants help to understand the structure–activity relationships of MEK inhibitors.

(2) Assays can be designed to favor compounds that bind at different sites and with different modes of action. This phenomenon can be exploited to identify compounds with diverse chemical and biological properties and so give alternative options for candidate drugs. The target protein kinase may be in a nonactivated or activated state; it could be in a balanced distribution between free enzyme and various intermolecular complexes that arises from selection of appropriate ligand concentrations.

ACKNOWLEDGMENT

We thank the following people for their contributions: Andy Barker, Tom Boyle, Graham Crawley, Keith Gibson, Laurent Hennequin, Christine Lambert, Ross Overman, and Phil Poyser. In particular, we remember Tom Boyle, who brought great knowledge and humor to our work.

SUPPORTING INFORMATION AVAILABLE

Further descriptions are given for the following experimental procedures: expression and purification of MEK1; synthesis of *N*-alkyl amide. This material is available free of charge via the Internet at http://pubs.acs.org.

REFERENCES

1. Manning, G., Whyte, D. B., Martinez, R., Hunter, T., and Sudarsanam, S. (2002) The protein kinase complement of the human genome. *Science 298*, 1912–1934.
2. Cohen, P. (2002) Protein kinases—the major drug targets of the 21st century? *Nat. Rev. Drug Discov. 1*, 309–315.
3. Cherry, M., and Williams, D. H. (2004) Recent kinase and kinase inhibitor X-ray structures: Mechanisms of inhibition and selectivity insights. *Curr. Med. Chem. 11*, 663–673.
4. Noble, M. E. M., Endicott, J. A., and Johnson, L. N. (2004) Protein kinase inhibitors: insights into design from structure. *Science 303*, 1800–1805.
5. Knight, Z. A., and Shokat, K. M. (2005) Features of selective kinase inhibitors. *Chem. Biol. 12*, 621–637.
6. Sebolt-Leopold, J. E., and Herrera, R. (2004) Targeting the mitogen-activated protein kinase cascade to treat cancer. *Nat. Rev. Cancer 4*, 937–947.
7. Wallace, E. M., Lyssikatos, J. P., Yeh, T., Winkler, J. D., and Koch, K. (2005) Progress towards theraeutic small molecule MEK inhibitors for use in cancer therapy. *Curr. Top. Med. Chem. 5*, 215–229.
8. Favata, M. F., Horiuchi, K. Y., Manos, E. J., Daulerio, A. J., Stradley, D. A., Feeser, W. S., Van Dyk, D. E., Pitts, W. J., Earl, R. A., Hobbs, F., Copeland, R. A., Magolda, R. L., Scherle, P. A., and Trzaskos, J. M. (1998) Identification of a novel inhibitor of mitogen-activated protein kinase kinase. *J. Biol. Chem. 273*, 18623–18632.
9. Ahn, N. G., Nahreini, T. S., Tolwinski, N. S., and Resing, K. A. (2001) Pharmacologic inhibitors of MKK1 and MKK2. *Methods Enzymol. 332*, 417–431.
10. Mansour, S. J., Candia, J. M., Matsuura, J. E., Manning, M. C., and Ahn, N. G. (1996) Interdependent domains controlling the enzymatic activity of mitogen-activated protein kinase kinase 1. *Biochemistry 35*, 15529–15536.
11. Sebolt-Leopold, J. S., Dudley, D. T., Herrera, R., Van Becelaere, K., Wiland, A., Gowan, R. C., Tecle, H., Barrett, S. D., Bridges, A., Przybranowski, S., Leopold, W. R., and Saltiel, A. R. (1999) Blockade of the MAP kinase pathway suppresses growth of colon tumors *in vivo*. *Nat. Med. 5*, 810–816.
12. Ohren, J. F., Chen, H., Pavlovsky, A., Whitehead, C., Zhang, E., Kuffa, P., Yan, C., McConnell, P., Spessard, C., Banotai, C., Mueller, W. T., Delaney, A., Omer, C., Sebolt-Leopold, J., Dudley, D. T., Leung, I. K., Flamme, C., Warmus, J., Kaufman, M., Barrett, S., Tecle, H., and Hasemann, C. A. (2004) Structures of human MAP kinase kinase 1 (MEK1) and MEK2 describe novel non-competitive kinase inhibition. *Nat. Struct. Mol. Biol. 11*, 1192–1197.
13. Barrett, S. D., Bridges, A. J., Doherty, A. M., Dudley, D. T., Saltiel, A. R., and Tecle, H. (1999) Preparation of 4-bromo or 4-iodo phenylamino benzhydroxamic acid derivatives as MEK inhibitors, International Patent, WO 99/01426.
14. Boyle, F. T., Gibson, K. H., Poyser, J. P., and Turner, P. (2000) Preparation of quinoline derivatives as inhibitors of MEK enzymes, International Patent, WO 00/068201.
15. Boyle, F. T., Gibson, K. H., and Foote, K. M. (2002) Substituted quinolines as antitumour agents, International Patent, WO 02/044166.
16. Crawley, G. C., McKerrecher, D., Poyser, J. P., Hennequin, L. F., Plé, P., and Lambert, C. M.-P. (2001) Quinazoline derivatives, International Patent, WO 01/04102.
17. Sullivan, J. E., Holdgate, G. A., Campbell, D., Timms, D., Gerhardt, S., Breed, J., Breeze, A. L., Bermingham, A., Pauptit, R. A., Norman, R. A., Embrey, K. J., Read, J., VanScyoc, W. S., and Ward, W. H. J. (2005) Prevention of MKK6-dependent activation by binding to p38α MAP kinase. *Biochemistry 44*, 16475–16490.
18. Mannervik, B. (1982) Regression analysis, experimental error, and statistical criteria in the design and analysis of experiments for discrimination between rival kinetic models. *Methods Enzymol. 87*, 370–390.
19. Segel, I. H. (1975) *Enzyme Kinetics*, pp 203−206, John Wiley & Sons, New York.
20. Cheng, Y.-C., and Prusoff, W. H. (1973) Relationship between the inhibition constant and the concentration of inhibitor which causes 50% inhibition (I_{50}) of an enzymatic reaction. *Biochem. Pharmacol. 22*, 3099–3108.
21. Prowse, C. N., Hagopian, J. C., Cobb, M. H., Ahn, N. G., and Lew, J. (2000) Catalytic reaction pathway for the mitogen-activated protein kinase ERK2. *Biochemistry 39*, 6258–6266.
22. Smith, C. K., and Windsor, W. T. (2007) Thermodynamics of nucleotide and non-ATP-competitive inhibitor binding to MEK1 by circular dichroism and isothermal titration calorimetry. *Biochemistry 46*, 1358–1367.
23. Feng, B. Y., Shelat, A., Doman, T. N., Guy, R. K., and Shoichet, B. K. (2005) High-throughput assays for promiscuous inhibitors. *Nat. Chem. Biol. 1*, 146–148.
24. Davies, S. P., Reddy, H., Caiavano, M., and Cohen, P. (2000) Specificity and mechanism of action of some commonly used protein kinase inhibitors. *Biochem. J. 351*, 95–105.
25. Duncia, J. V., Santella, J. B., III, Higley, C. A., Pitts, W. J., Wityak, J., Frietze, W. E., Rankin, F. W., Sun, J. H., Earl, R. A., Tabaka, A. C., Teleha, C. A., Blom, K. F., Favata, M. F., Manos, E. J., Daulerio, A. J., Stradley, D. A., Horiuchi, K., Copeland, R. A., Scherle, P. A., Trzaskos, J. M., Magolda, R. L., Trainor, G. L., Wexler, R. R., Hobbs, F. W., and Olson, R. E. (1998) MEK inhibitors: the chemistry and biological activity of U-0126, its analogs, and cyclization products. *Bioorg. Med. Chem. Lett. 8*, 2839–2844.
26. Horiuchi, K. Y., Scherle, P. A., Trzaskos, J. M., and Copeland, R. A. (1998) Competitive inhibition of MAP kinase activation by a peptide representing the alpha C helix of ERK. *Biochemistry 37*, 8879–8885.
27. Nagar, B., Hantschel, O., Young, M. A., Scheffzek, K., Veach, D., Bondman, W., Clarkson, B., Superti-Furga, G., and Kuriyan, J. (2003) Structural basis for the autoinhibition of c-Abl tyrosine kinase. *Cell 112*, 859–871.
28. Atwell, S., Adams, J. M., Badger, J., Buchanan, M. D., Feil, I. K., Froning, K. J., Gao, X., Hendle, J., Keegan, K., Leon, B. C., Muller-Dieckmann, H. J., Nienaber, V. L., Noland, B. W., Post, K., Rajashankar, K. R., Ramos, A., Russell, M., Burley, S. K., and Buchanan, S. G. (2004) A novel mode of Gleevec binding is revealed by the structure of spleen tyrosine kinase. *J. Biol. Chem. 279*, 55827–55832.
29. Davidson, W., Frego, L., Peet, G. W., Kroe, R. R., Labadia, M. E., Lukas, S. M., Snow, R. J., Jakes, S., Grygon, C. A., Pargellis, C., and Werneburg, B. G. (2004) Discovery and characterization of a substrate selective p38α inhibitor. *Biochemistry 43*, 11658–11671.
30. Duntiz, J. D. (1995) Win some, lose some: enthalpy-entropy compensation in weak intermolecular interactions. *Chem. Biol. 2*, 709–712.
31. Engh, R. A., Girod, A., Kinzel, V., Huber, R., and Bossemeyer, D. (1996) Crystal structures of catalytic subunit of cAMP-dependent protein kinase in complex with isoquinolinesulfonyl protein kinase inhibitors H7, H8, and H89. Structural implications for selectivity. *J. Biol. Chem. 271*, 26157–26164.
32. Collins, I., Caldwell, J., Fonseca, T., Donald, A., Bavetsias, V., Hunter, L.-J. K., Garrett, M. D., Rowlands, M. G., Aherne, G. W.,

Davies, T. G., Berdini, V., Woodhead, S. J., Davis, D., Seavers, L. C. A., Wyatt, P. G., Workman, P., and McDonald, E. (2006) Structure-based design of isoquinoline-5-sulfonamide inhibitors of protein kinase B. *Bioorg. Med. Chem. 14*, 1255–1273.

33. Hartshorn, M. J., Murray, C. W., Cleasby, A., Frederickson, M., Tickle, I. J., and Jhoti, H. (2005) Fragment-based lead discovery using X-ray crystallography. *J. Med. Chem. 48*, 403–413.
34. Hajduk, P. J., Bures, M., Praestgaard, J., and Fesik, S. W. (2000) Privileged molecules for protein binding identified from NMR-based screening. *J. Med. Chem. 43*, 3443–3447.
35. Lo, M.-C., Aulabaugh, A., Jin, G., Cowling, R., Bard, J., Malamas, M., and Ellestad, G. (2004) Evaluation of fluorescence-based thermal shift assays for hit identification in drug discovery. *Anal. Biochem. 332*, 153–159.
36. Muckenschnabel, I., Falchetto, R., Mayr, L. M., and Filipuzzi, I. (2004) SpeedScreen: label-free liquid chromatography-mass spectrometry-based high-throughput screening for the discovery of orphan protein ligands. *Anal. Biochem. 324*, 241–249.
37. Fabian, M. A., III, Treiber, D. K., Atteridge, C. E., Azimioara, M. D., Benedetti, M. G., Carter, T. A., Ciceri, P., Edeen, P. T., Floyd, M., Ford, J. M., Galvin, M., Gerlach, J. L., Grotzfeld, R. M., Herrgard, S., Insko, D. E., Insko, M. A., Lai, A. G., Lelias, J. M., Mehta, S. A., Milanov, Z. V., Velasco, A. M., Wodicka, L. M., Patel, H. K., Zarrinkar, P. P., and Lockhart, D. J. (2005) A small molecule-kinase interaction map for clinical kinase inhibitors. *Nat. Biotechnol. 23*, 329–336.
38. Swinney, D. C. (2006) Biochemical mechanisms of new molecular entities (NMEs) approved by United States FDA during 2001–2004: mechanisms leading to optimal efficacy and safety. *Curr. Top. Med. Chem. 6*, 461–478.

BI701811X